

July 26, 2023

**Yongfeng Zhang**  
Assistant Professor  
University of Wisconsin Madison

# Statistical modeling of the effect of microstructural heterogeneity on the irradiation behavior of TRISO fuel buffer layer

NEUP: 20-19556

PI: Yongfeng Zhang, University of Wisconsin Madison (UW), [yzhang2446@wisc.edu](mailto:yzhang2446@wisc.edu)

Co-PIs: Ramathasan Thevamaran (UW), Karim Ahmed (TAMU), Tyler Gerczak (ORNL), Wen Jiang (INL)

Funding: \$800,000

Period: 10/1/2020 – 9/30/2023 (with NCE to 6/30/2024)

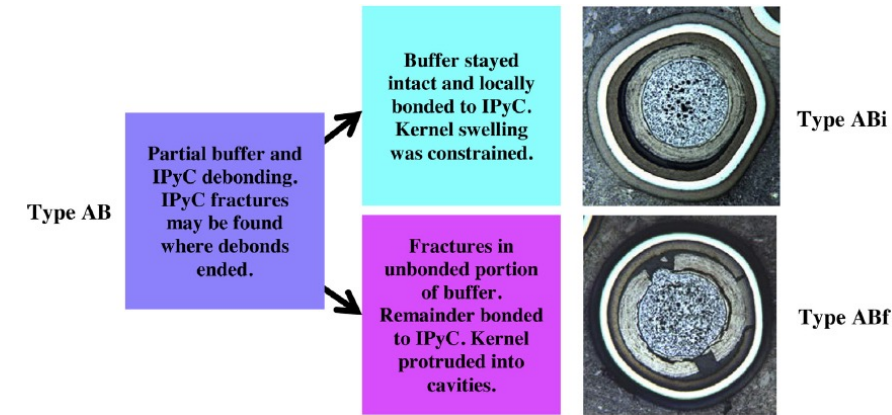
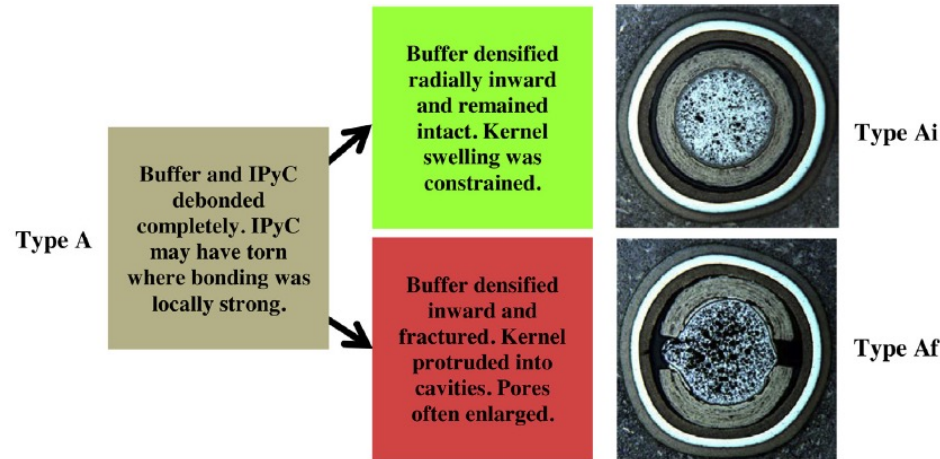


# Outline

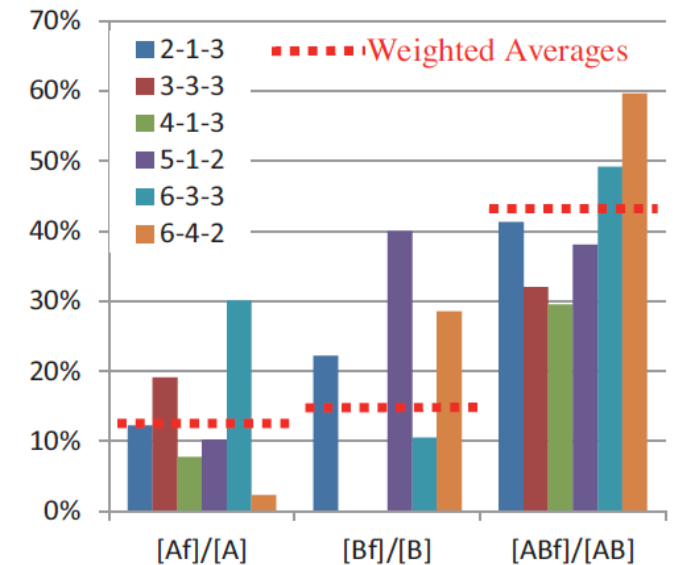
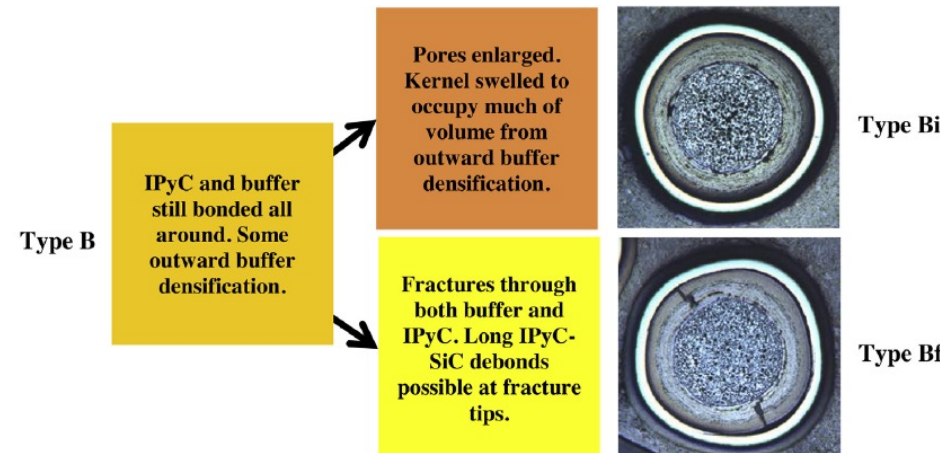
- **Background & objective**
- **Hypothesis**
- **Research design**
- **Accomplishments**
  - How do we describe buffer? matrix microstructure + porosity
  - How does buffer porosity affect its fracture behavior?
  - Irradiation induced changes in porosity and matrix microstructure
  - Super-elasticity of unirradiated buffer pyrocarbon
- **Outlook**
- **Summary**

# Background & objective

- Buffer fracture is stochastic showing three different modes: Debonding (A), radial fracture (B), and partial debonding (AB), while mode AB leads to higher probability of failure.



- **Our objective is to answer:**
  - Why fracture is stochastic?
  - What governs the selection of fracture mode?
  - Can we control the fracture mode?

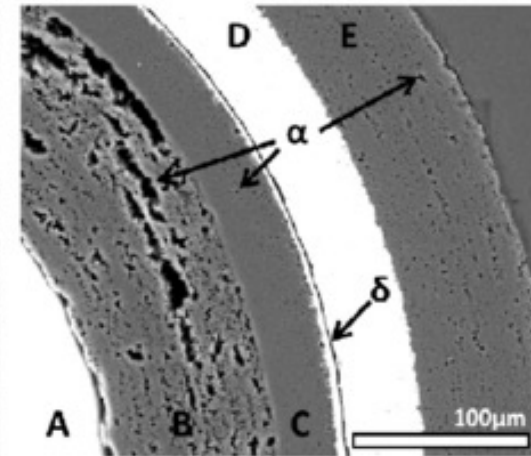
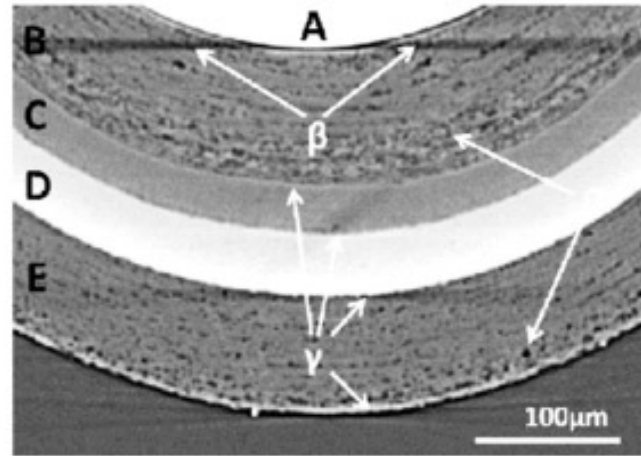




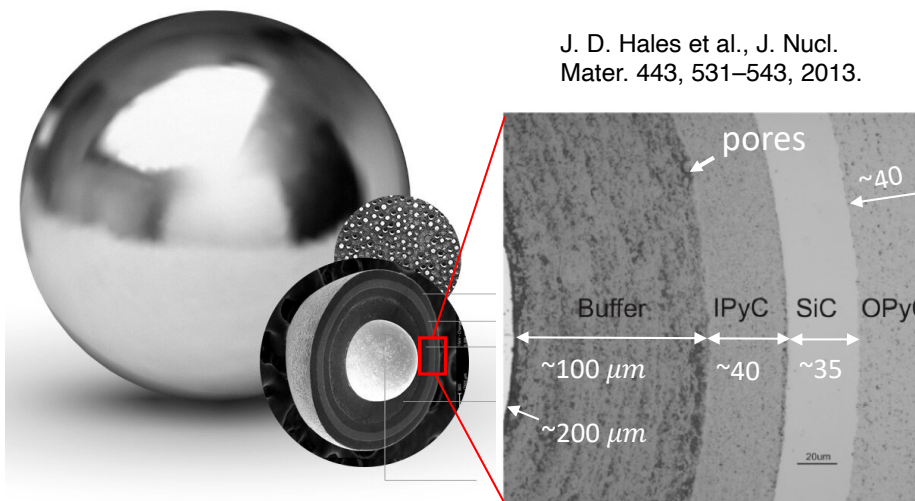
# Hypothesis: The heterogeneous distribution of buffer porosity determines the initiation and propagation of buffer fracture.

## Buffer porosity:

- Random distribution
- Local fluctuation
- Radially increasing
- Connectivity along tangential direction

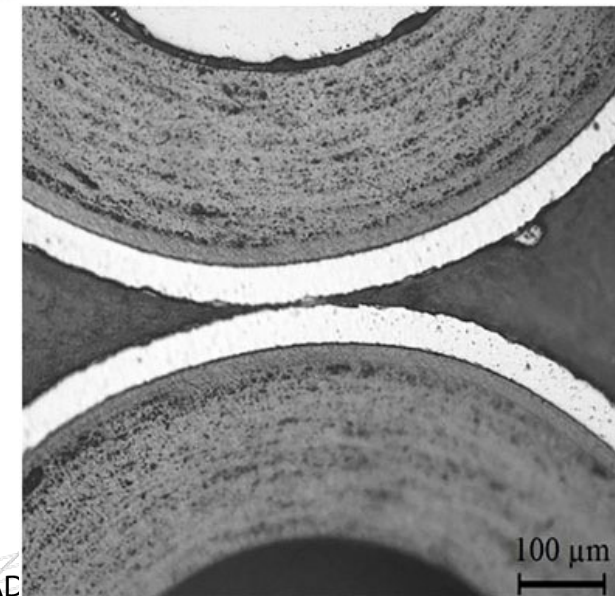


T. Lowe et al. JNM 461, 29-352015



J. D. Hales et al., J. Nucl. Mater. 443, 531–543, 2013.

S. Liu et al. Front. Mater., 04 January 2023

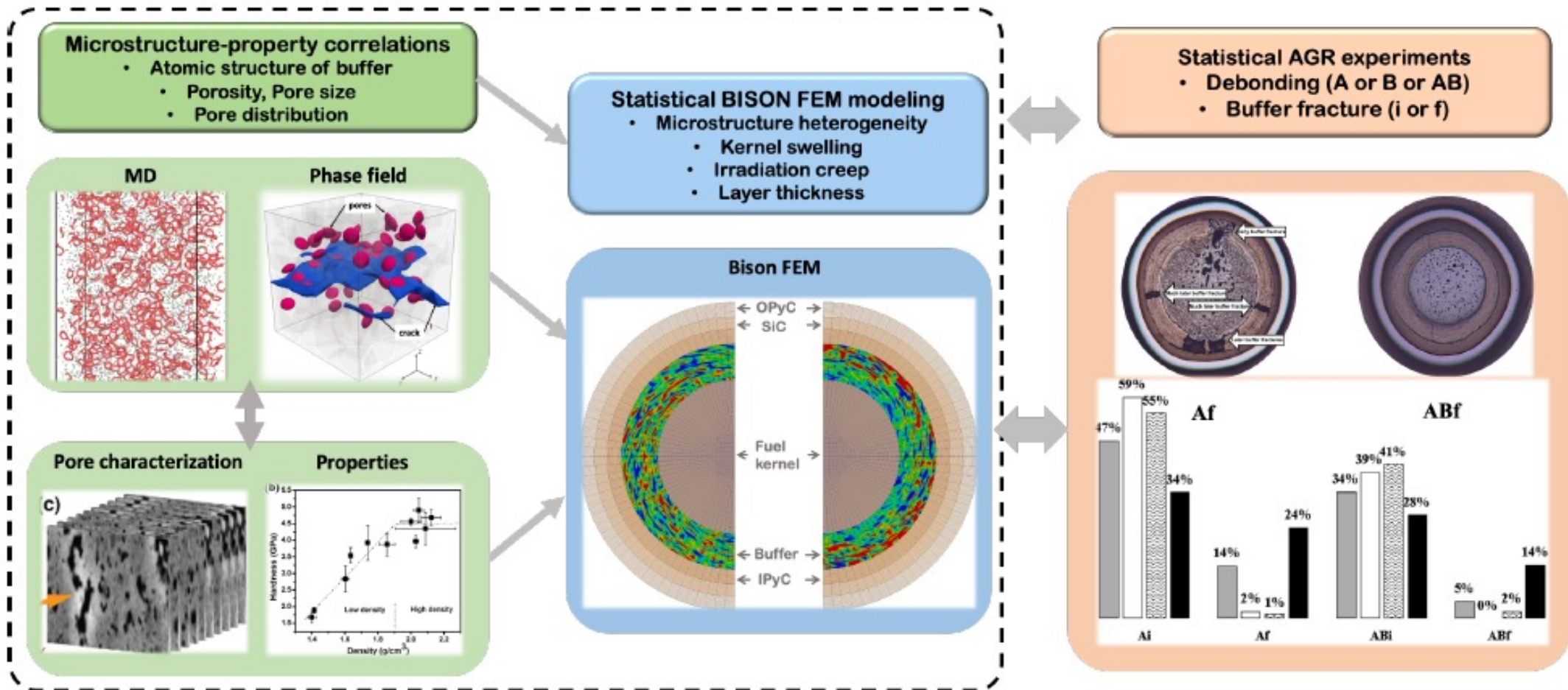


AC



# Research design

- What are the actual porosity in buffer and its spatial distribution?
- What's the atomic structure of buffer, which is a low density, non-textured pyrocarbon?
- How does porosity correlate with mechanical properties: moduli, toughness, etc.?
- How does porosity distribution affect the buffer fracture (tearing)?





# How do we describe buffer?

- **FIB-SEM characterization of buffer porosity**

- *Griesbach et al. Microstructural heterogeneity of the buffer layer of TRISO nuclear fuel particles, JNM 574 (2022)*

**1<sup>st</sup> place Winner of FY 2023 Innovations in Nuclear R&D Student Competition: Fuel Cycle Technologies**

- **Atomistic simulations of pyrocarbon matrix**

- *R. David et al. Correlations between atomic structure and elastic properties in low-density non-textured pyrocarbon (in preparation)*

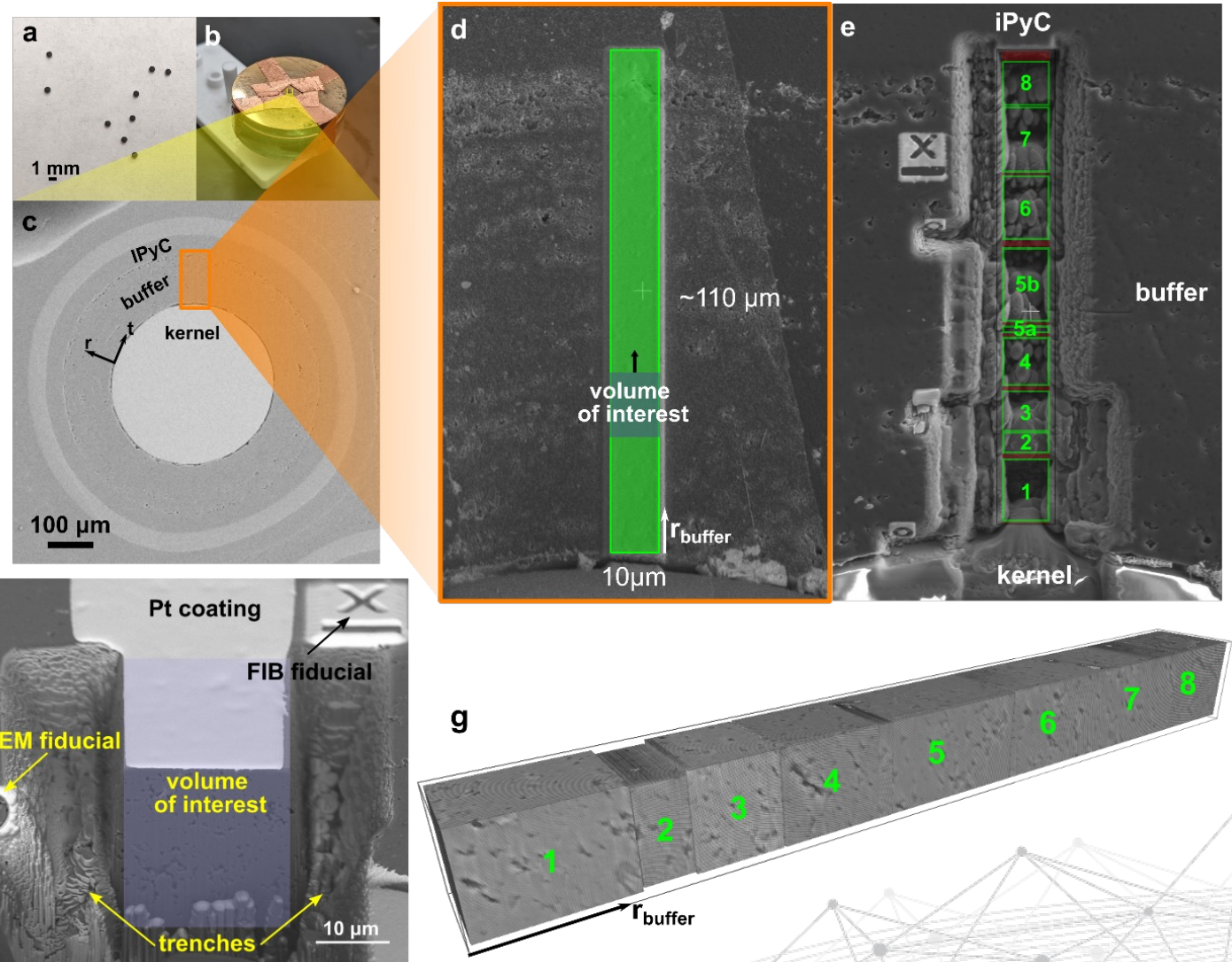


# Buffer porosity morphology in unirradiated TRISO buffer (surrogate particles)

A robust data analysis workflow is established incorporating artificial intelligence assisted pore identification and segmentation for porosity characterization of FIB-SEM image.

## FIB-SEM tomography

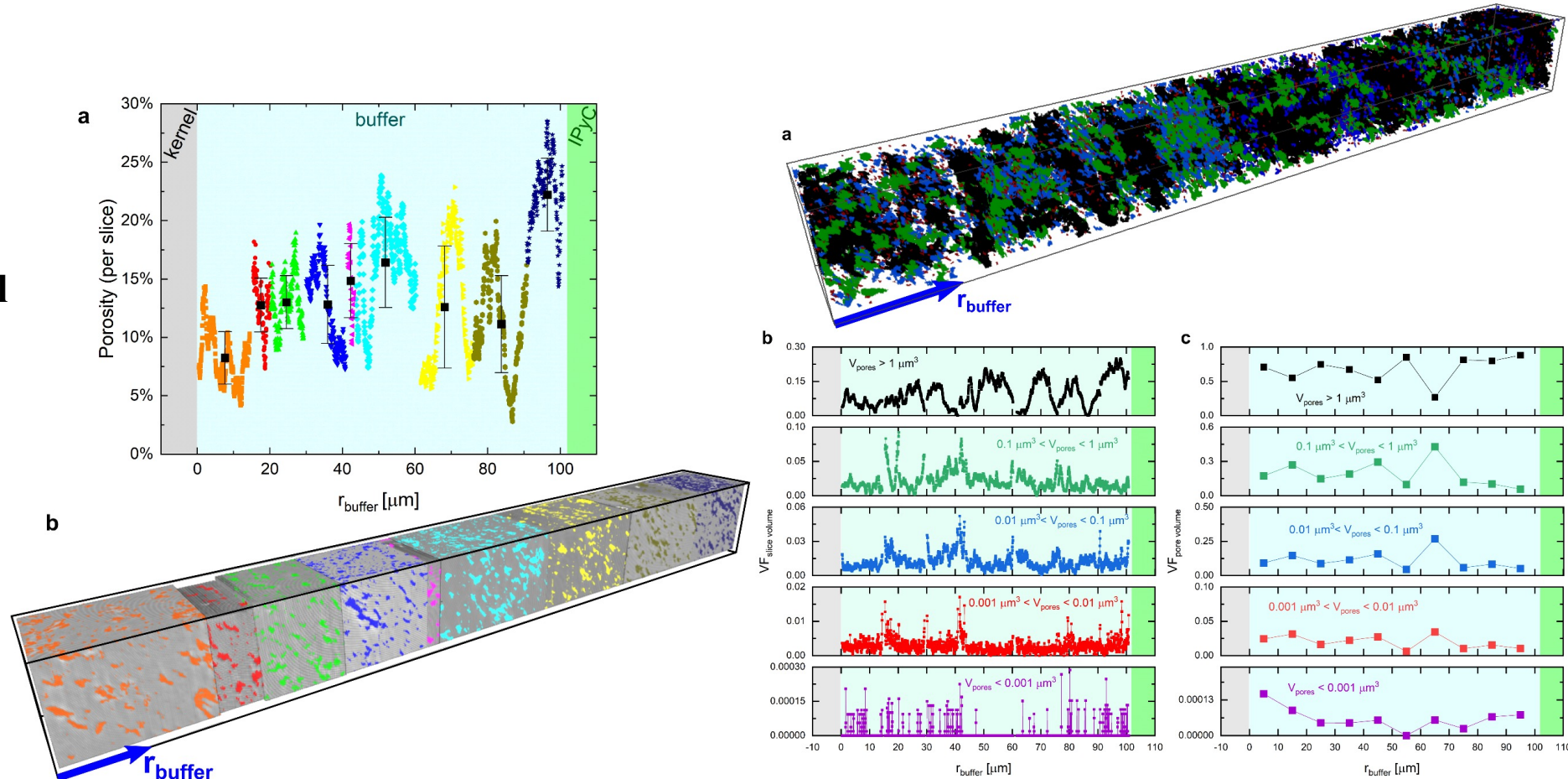
- FEI Helios PFIB with 30 kV Xe plasma
- Scan volume:  $10 \times 10 \times 10 \mu\text{m}^3$
- Slice thickness: 50 nm
- Voxel size:  $38 \times 49 \times 50 \text{ nm}^3$
  
- Image processing and data analyses:
  - Avizo 9.5 and Dragonfly 2021.1
  - Deep learning segmentation
  
- 3D reconstruction





# Buffer: low density pyrocarbon + randomly distributed pores

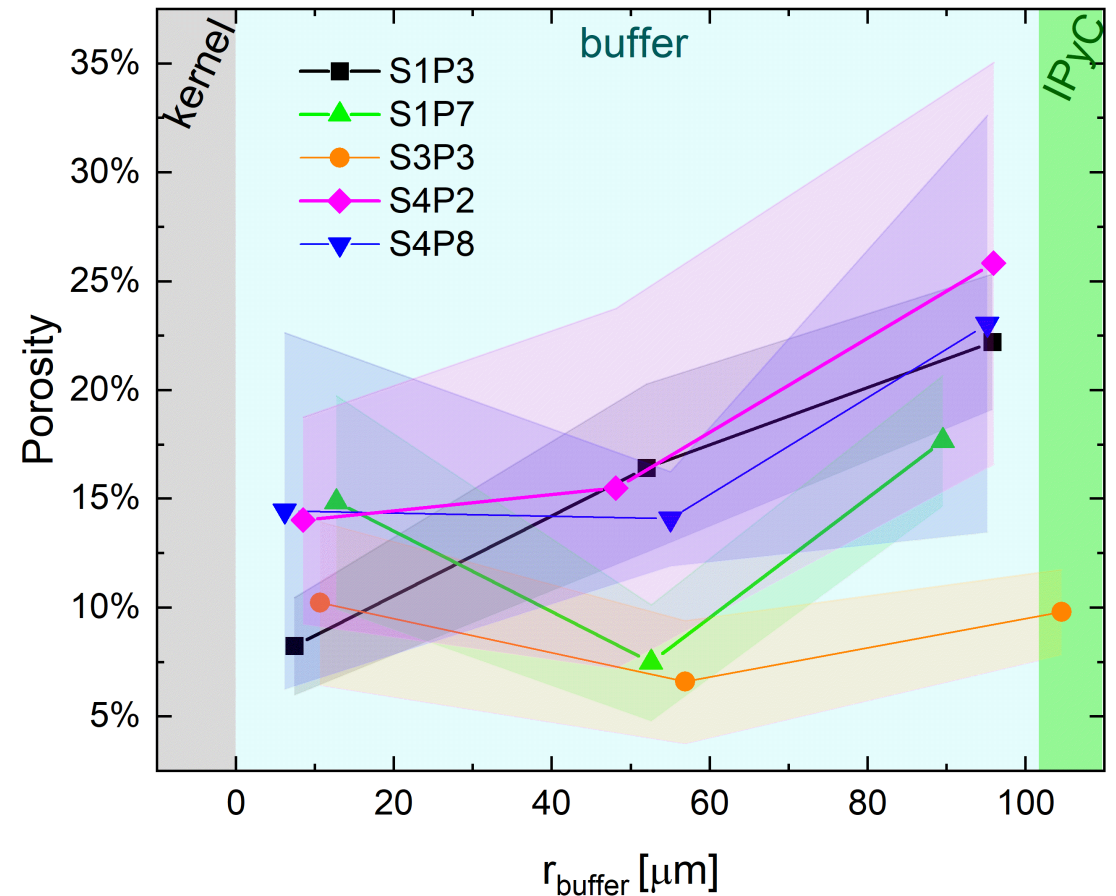
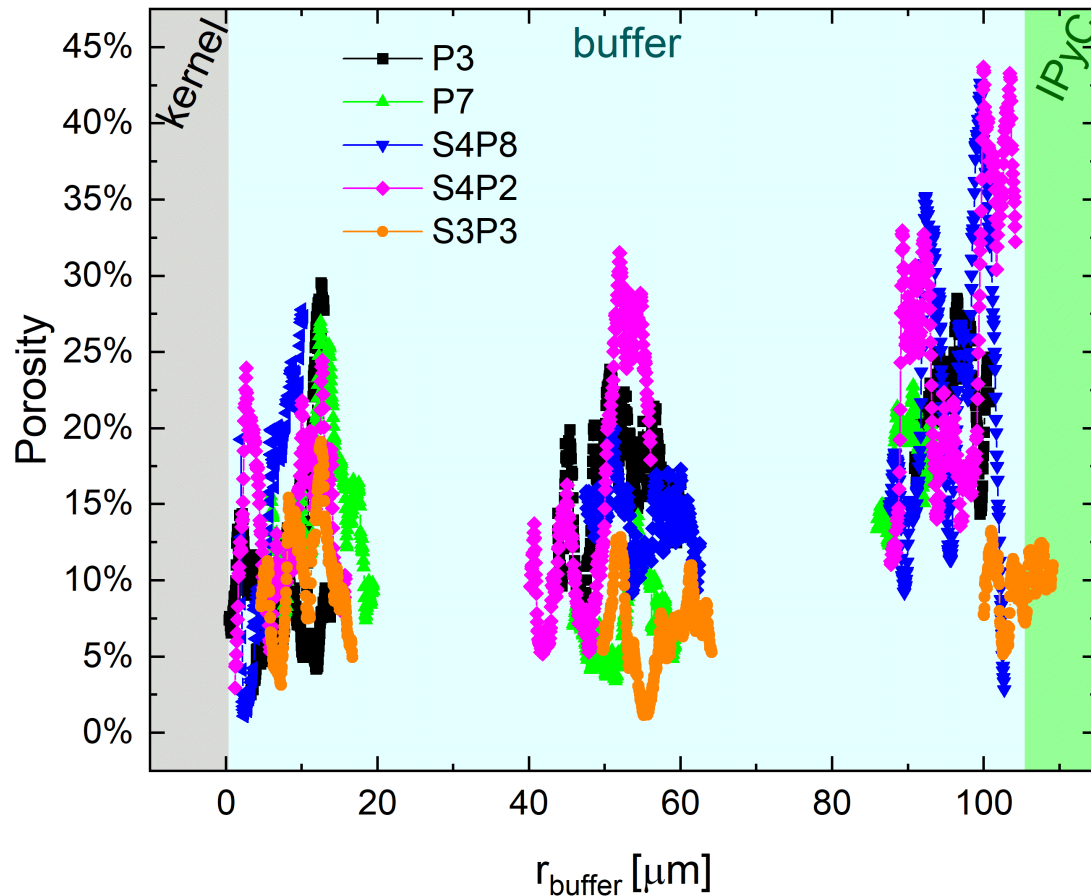
- The Average buffer porosity is about 14% in reference to the 50% smeared theoretical density.
- Pores distribute randomly.
- Porosity increases radially.
- Porosity fluctuates locally.
- Large pores ( $>1\mu m^3$ ) dominates the porosity albeit fewer of them.



Buffer consists of low density pyrocarbon with 58% theoretical density and randomly distributed pores that give a total porosity of 14%.

# Inter-particle (and radial direction) differences

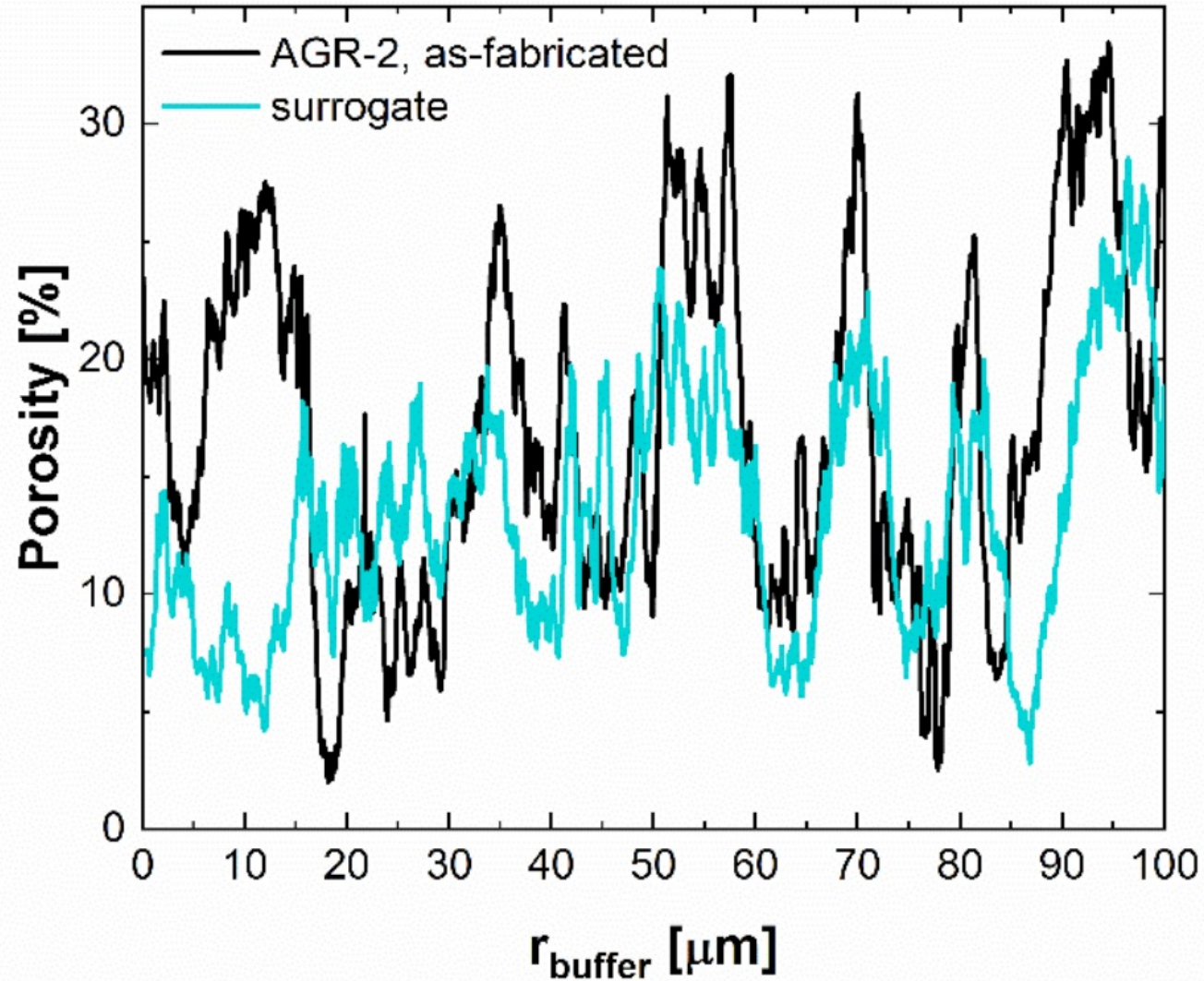
- The radial porosity distribution varies upon the radial direction and from particle to particle
- However, the average porosity, magnitude of local fluctuation and radial gradient are similar.
- The radial increase of porosity is consistent with the fabrication procedure.
- More characterizations (which are expensive) are desired.





# Difference between surrogate and AGR-2 TRISO particle

- Similar average porosity.
- Similar radial distribution.
- Larger fluctuation in the AGR-2 particle (?)

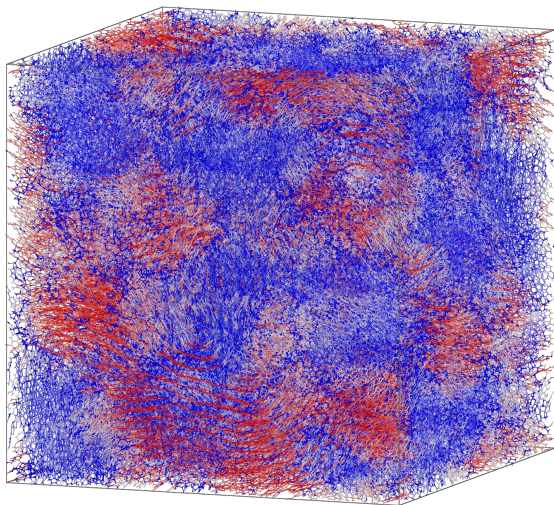




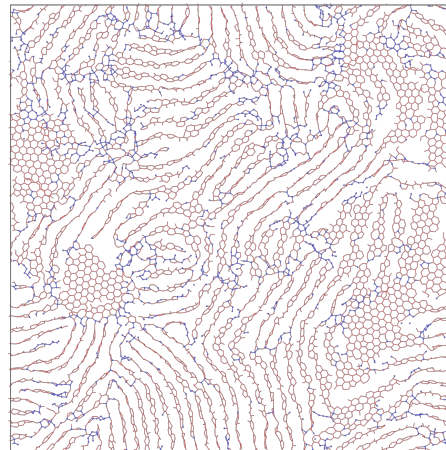
# Atomic structure of low density pyrocarbon

- Molecular dynamics simulations show that the low-density pyrocarbon is non-textured, containing randomly oriented graphite crystallites. Three parameters, **density**, and **in-plane** and **out-of-plane crystallite sizes**, are extracted from correlation analysis for describing the matrix microstructure.

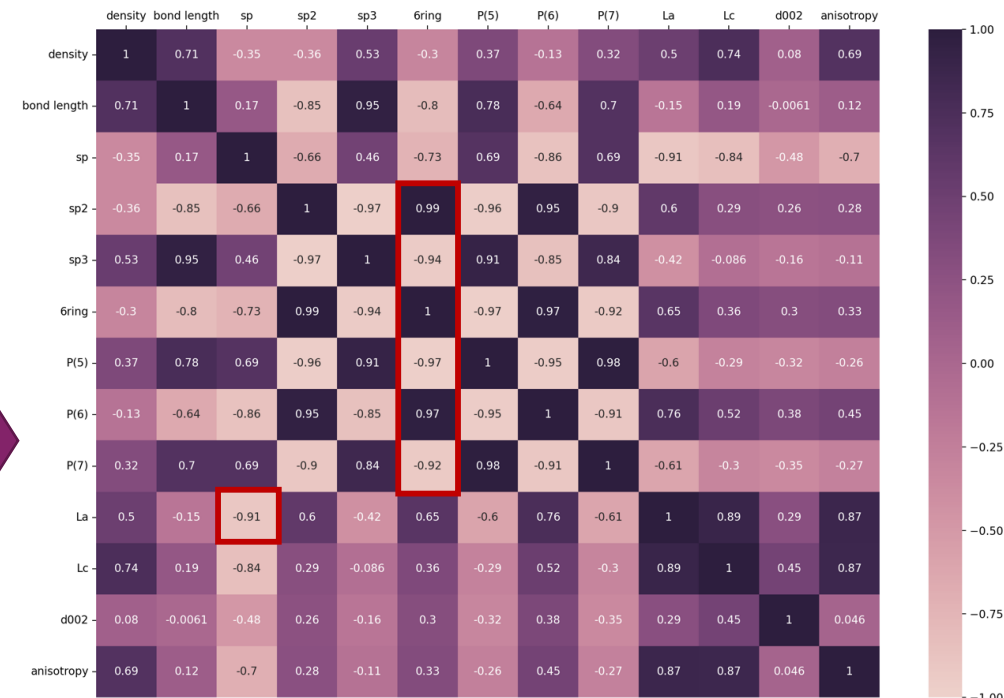
A 3D cell with atoms colored by atomic orientation



A slice in the cell with graphite-like atoms (red, sp<sup>2</sup> bonded and in 6-member rings) and defect (others)

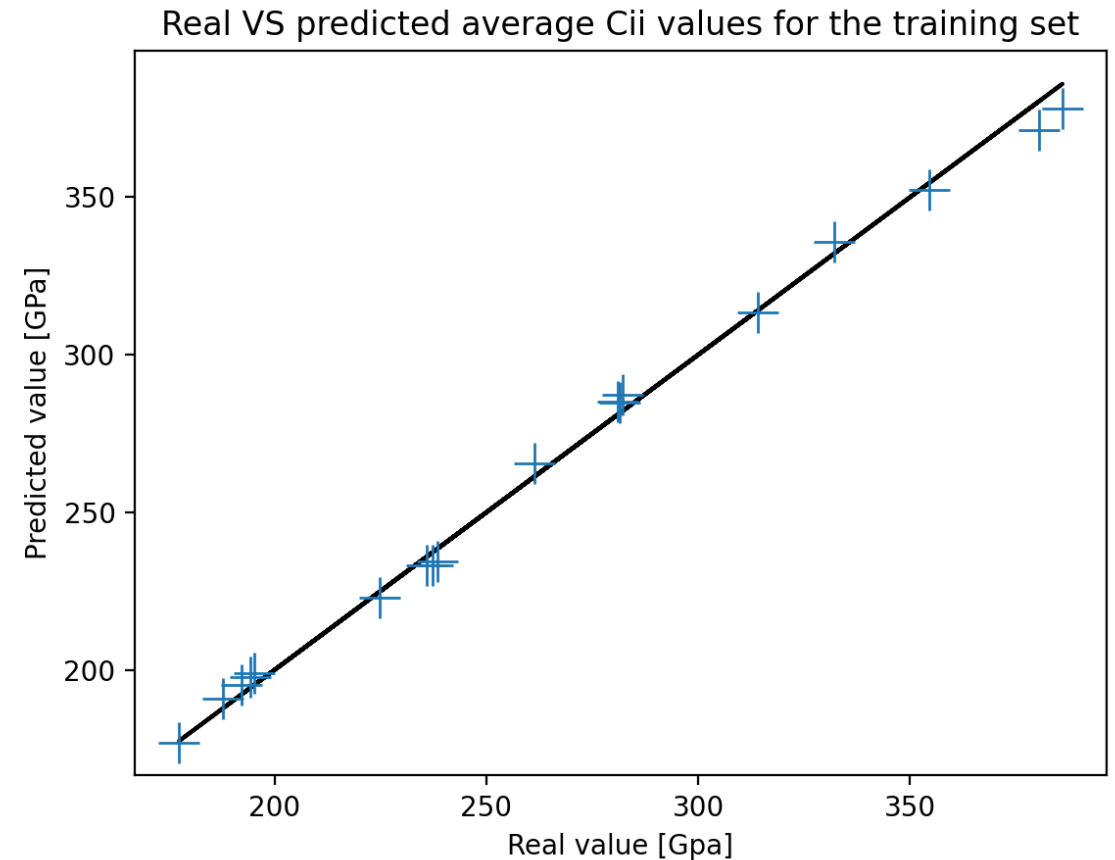



Correlations among descriptors



# Microstructure descriptors of buffer

- Porosity parameters
  - Average porosity
  - Radial gradient
  - Local fluctuation
  - Others?
- Matrix Parameters
  - Density
  - In-plane crystallite size  $L_a$
  - Out-of-plane crystallite size  $L_c$
  - Others?





# How does buffer porosity affect its fracture behavior?

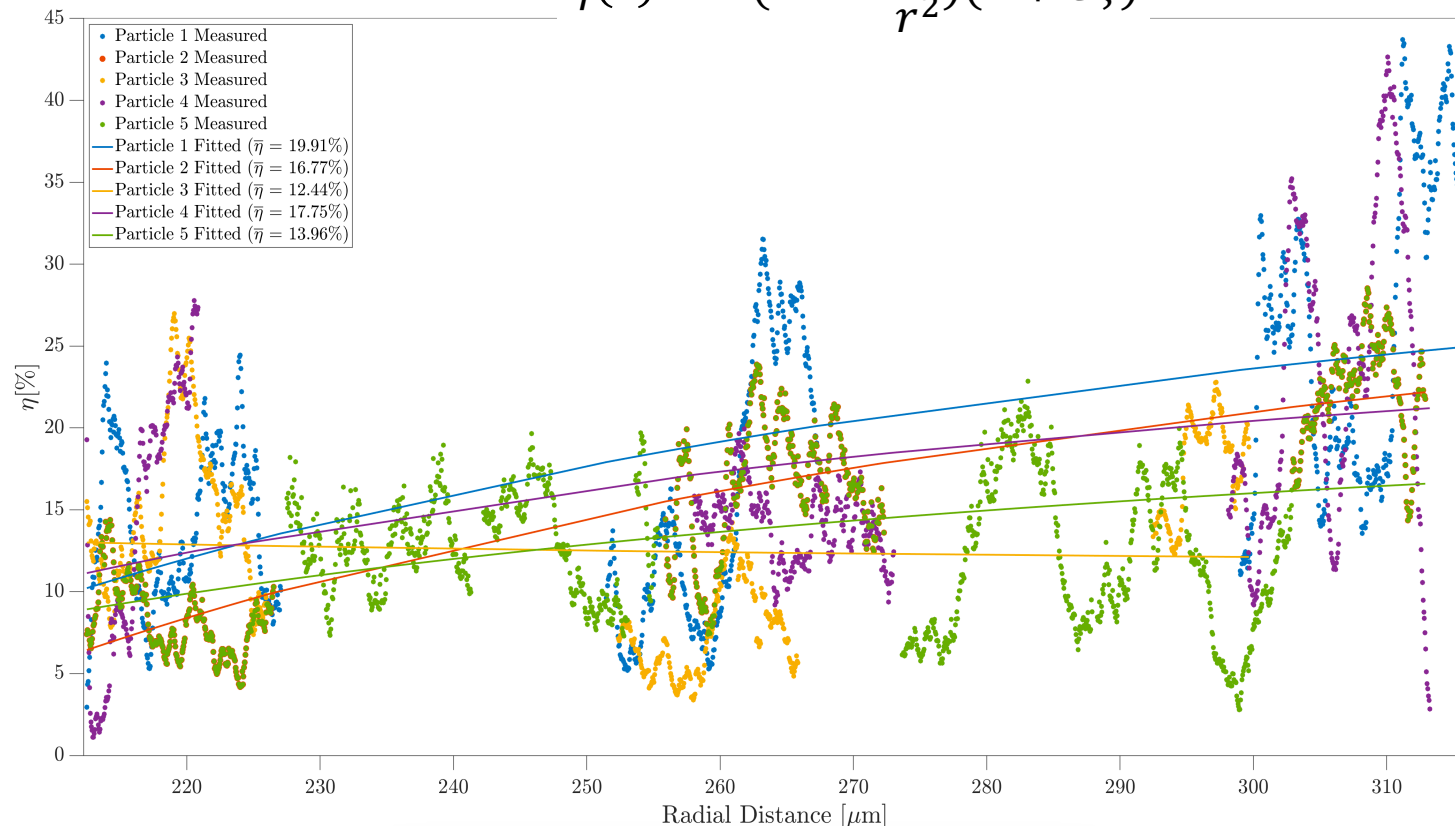
- **Statistical BISON simulations of buffer fracture initiation and propagation**
  - *Masri et al. The role of heterogeneous porosity distribution on buffer fracture behavior in TRISO fuel particles (in preparation)*



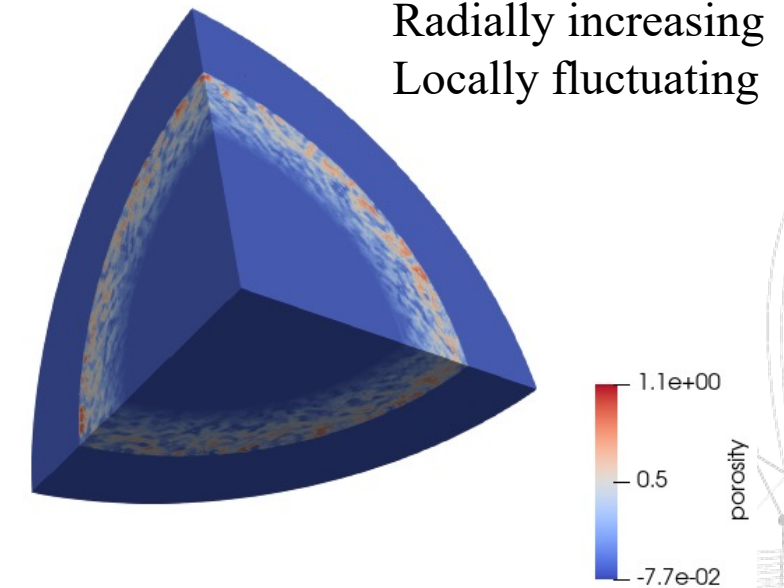
# Representation of buffer porosity in BISON

- Buffer porosity is randomly sampled with three parameters: **average porosity (A)**, **radial gradient (B)**, and **local fluctuation (Cξ)**, by fitting the experimental results using the below equation.
- The function is selected based on the assumption of constant mass deposition rate per unit radial length.
- Both elastic moduli and fracture stress are made dependent on porosity.

$$\eta(r) = A\left(1 - B \frac{r_0^2}{r^2}\right)(1 + C\xi)$$

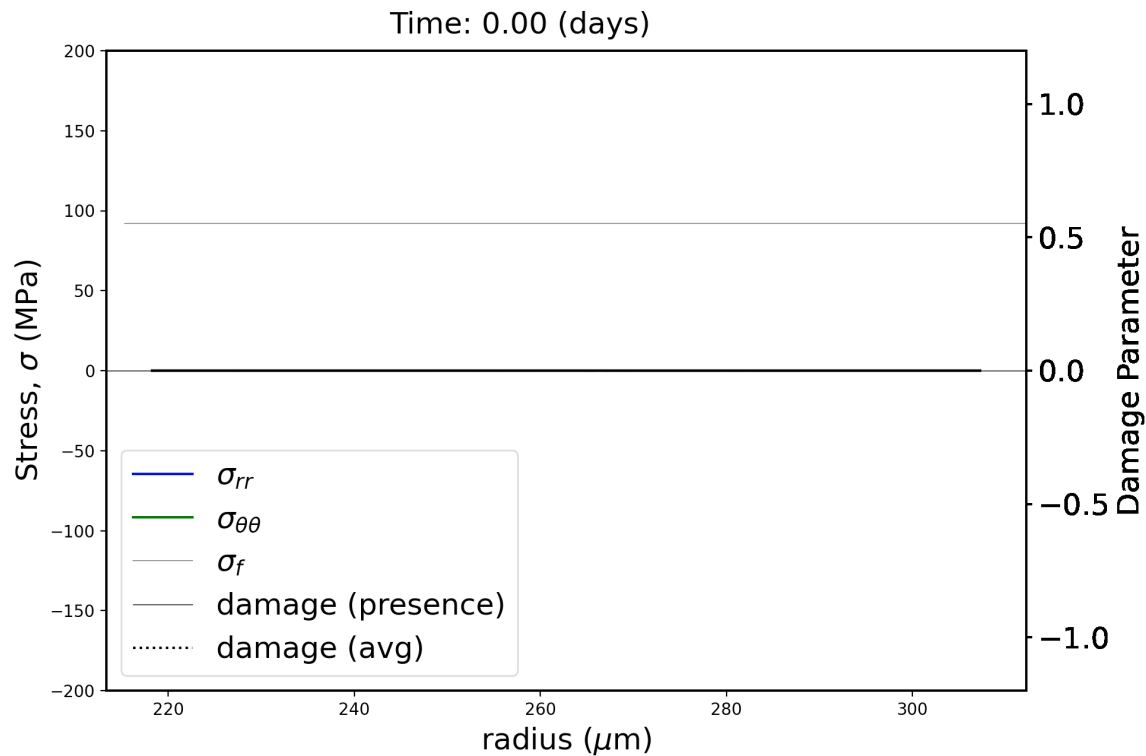


**BISON:** Williamson, R. L. et al., *J. Nucl. Mater.* 2012, 423 (1–3), 149–163.

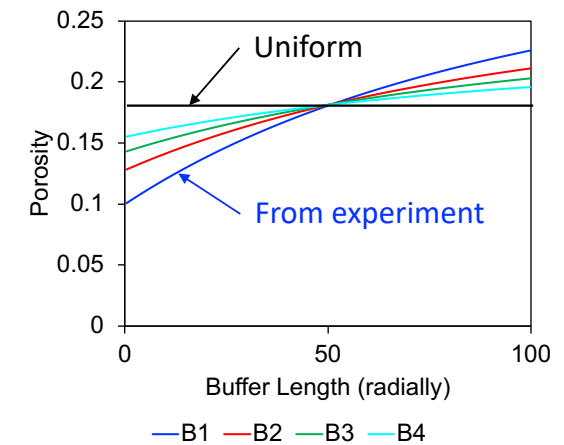
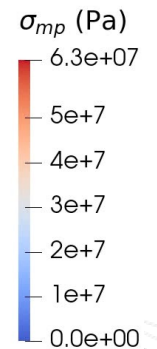
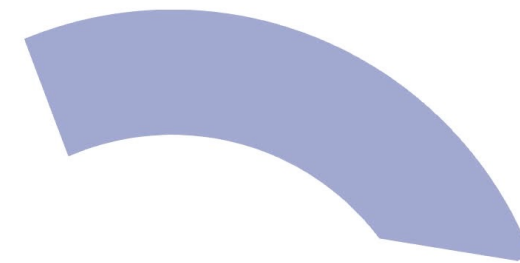


# BISON simulations of buffer fraction: uniform porosity

- Both elastic moduli and fracture stress are uniform
- Fracture is caused by tangential stress, not radial stress
- Fracture initiates from kernel/buffer interface
- Fracture propagates **radially**

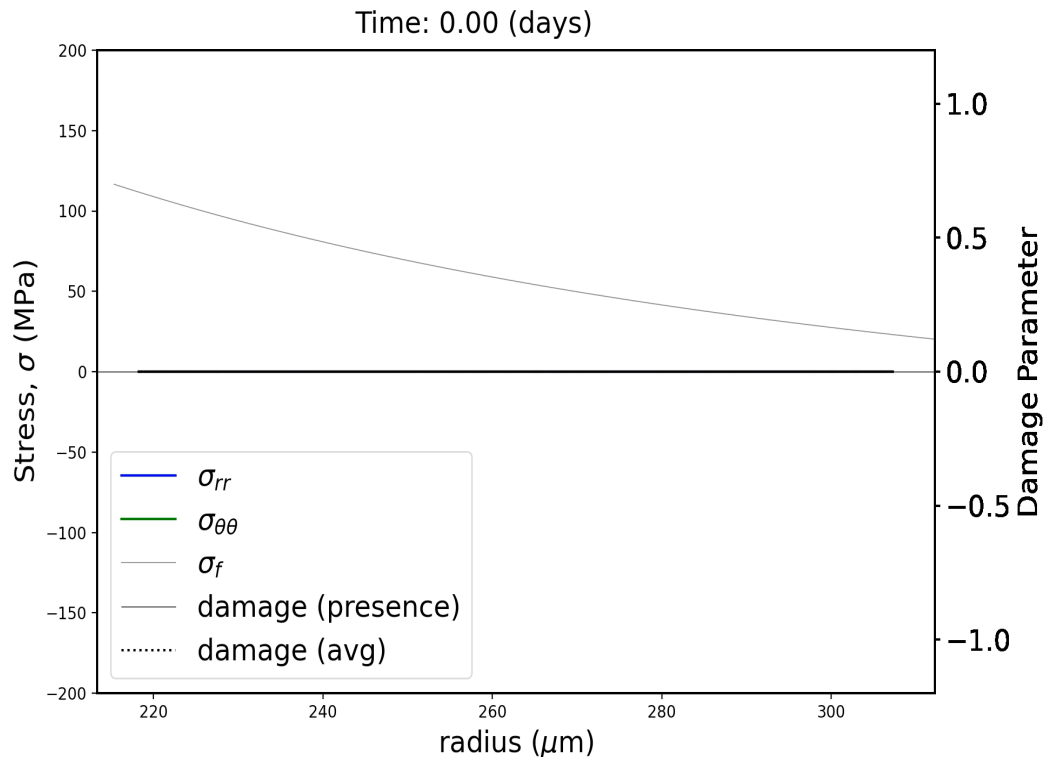
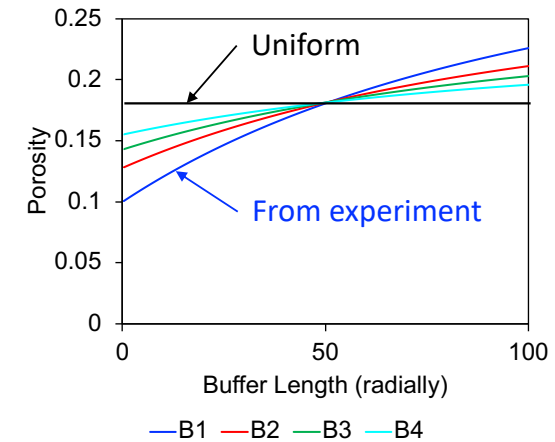


Color: stress  
Black: crack

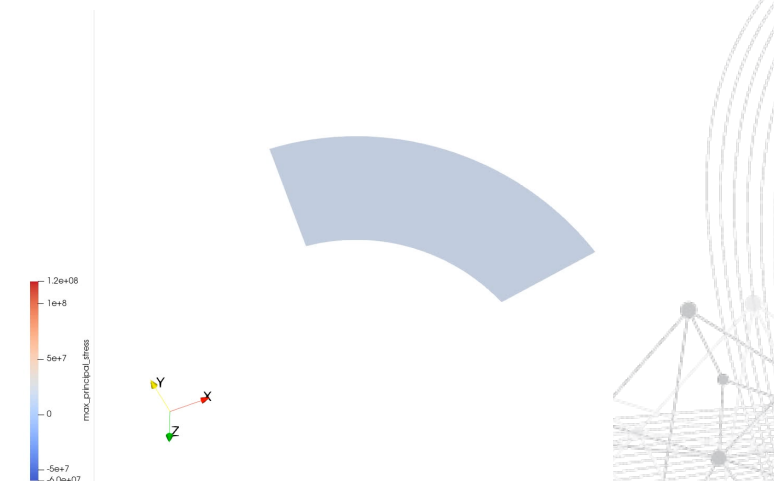


# BISON simulations of buffer fraction: radially increasing porosity

- Both elastic moduli and fracture stress decrease radially
- Fracture is caused by **tangential stress**, not radial stress
- Fracture initiates from **buffer/IPyC interface**
- Radial crack connects with each other along tangential direction (**tearing**), instead of propagating radially



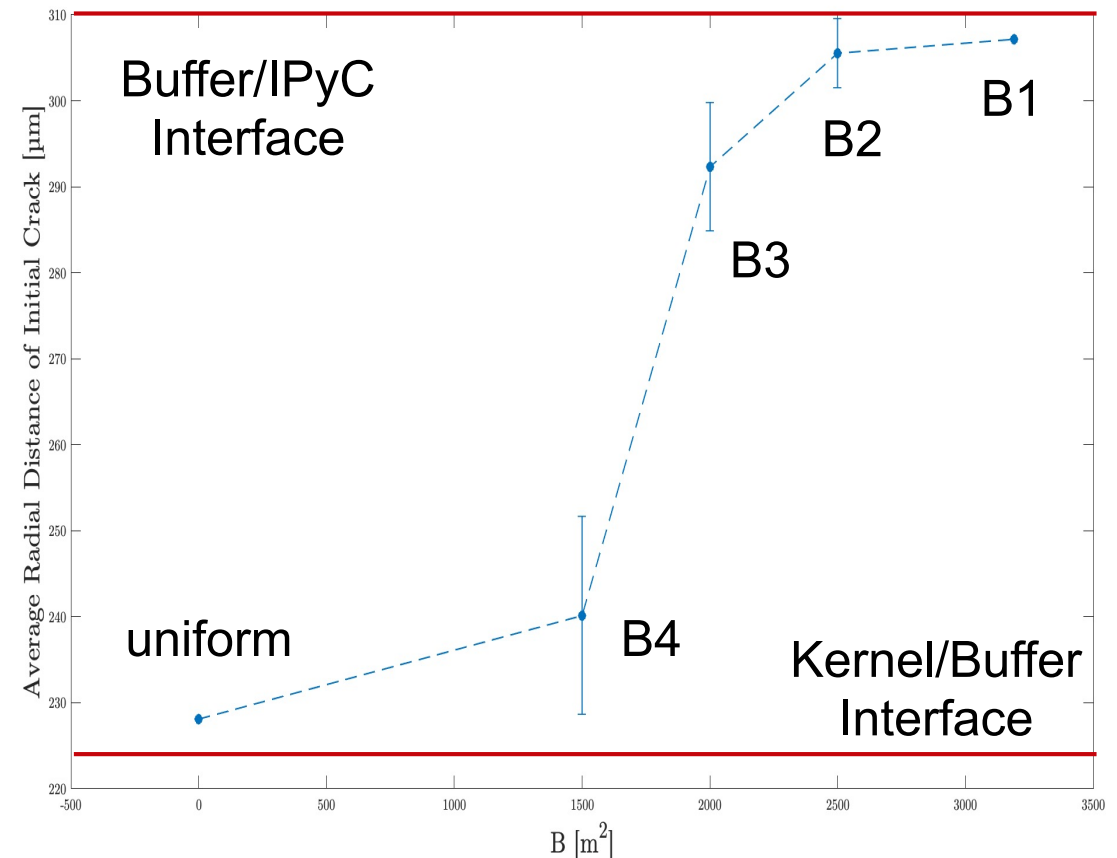
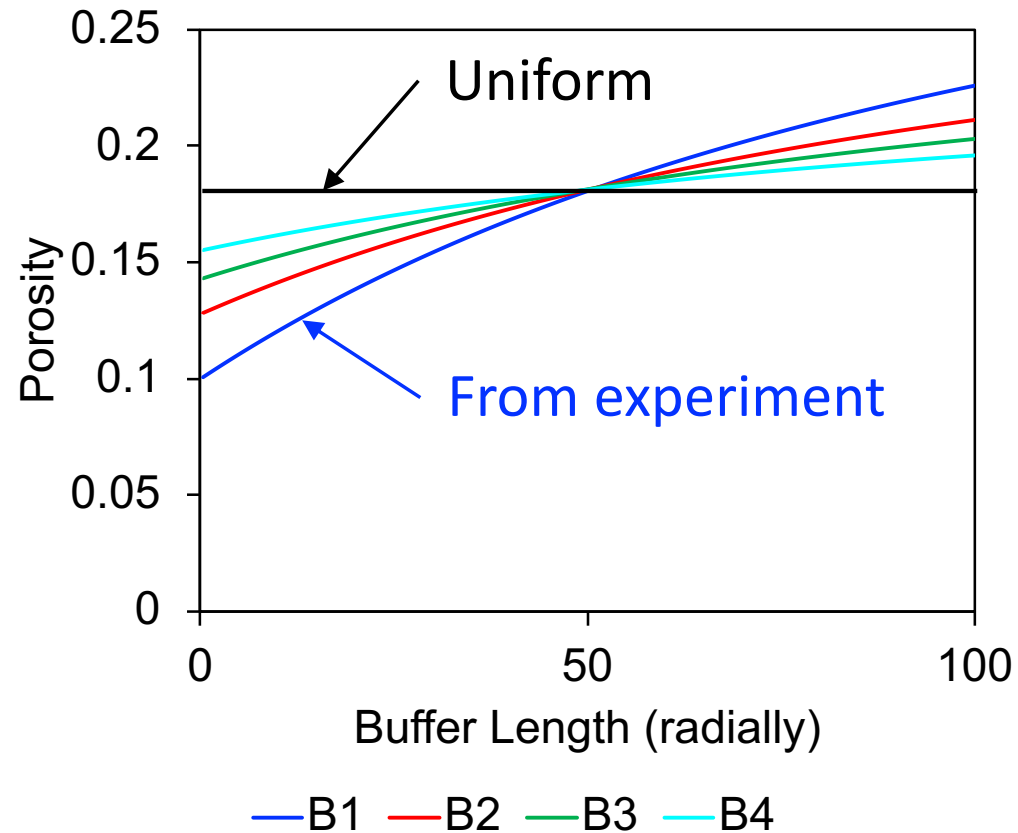
Color: stress  
Black: crack





# BISON simulations of buffer fracture: fracture initiation

- The fracture initiation point increases radially with the parameter B, which describes the rate of radial porosity increase, implying the possibility of tailoring fracture by controlling porosity distribution.
- Local fluctuation in porosity induces some fluctuation in fracture initiation point.





# Irradiation induced changes in porosity and matrix microstructure

## FIB-SEM characterization of buffer porosity

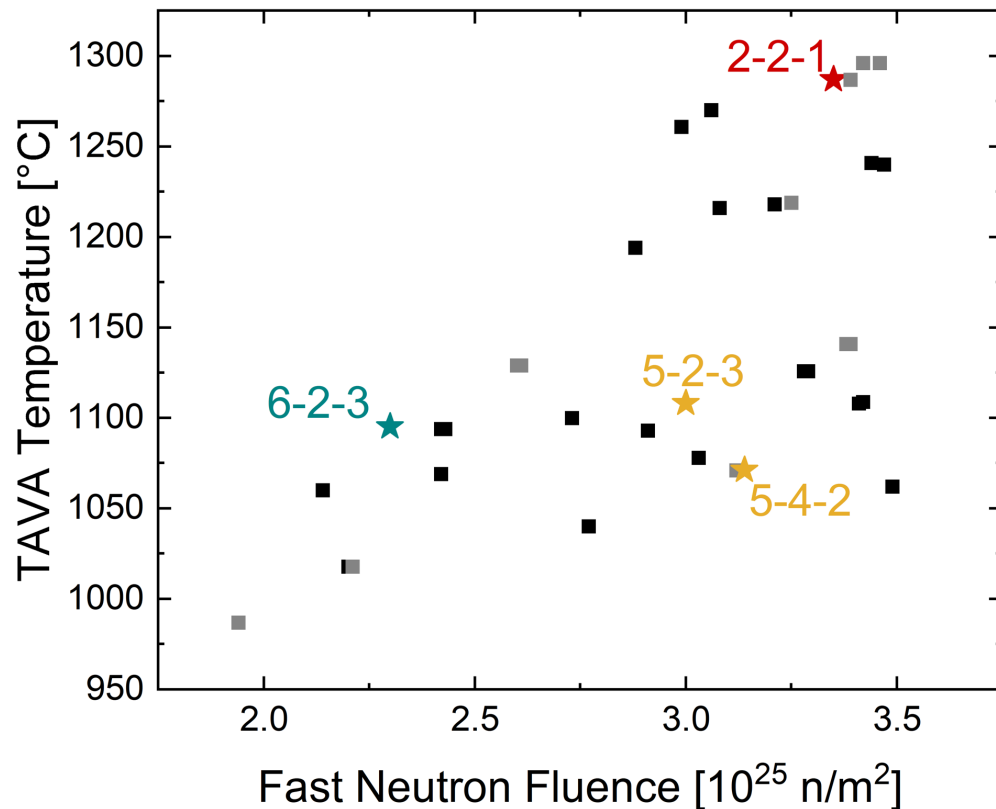
- *C. Griesbach, C. McKinney, Y. Zhang, T. Gerczak, R. Thevamaran, Irradiation-induced changes in the porous buffer microstructure of TRISO nuclear fuel particles (in preparation)*
- *C. Griesbach, J.D. Arregui Mena, E. Lopez, Y. Zhang, T. Gerczak, R. Thevamaran, Irradiation-induced nanostructural changes in porous pyrocarbon (in preparation)*

# Samples and irradiation condition

- Various irradiation conditions consider in terms of temperature and neutron fluence.
- **Porosity, solid fission products, densification, and fracture** are characterized.

5 - 4 - 2  
 capsule compact stack

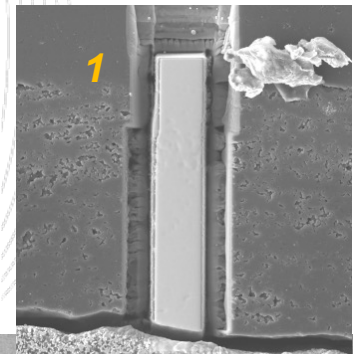
AGR-2 Irradiation Conditions



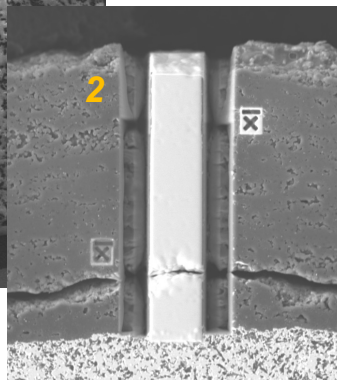
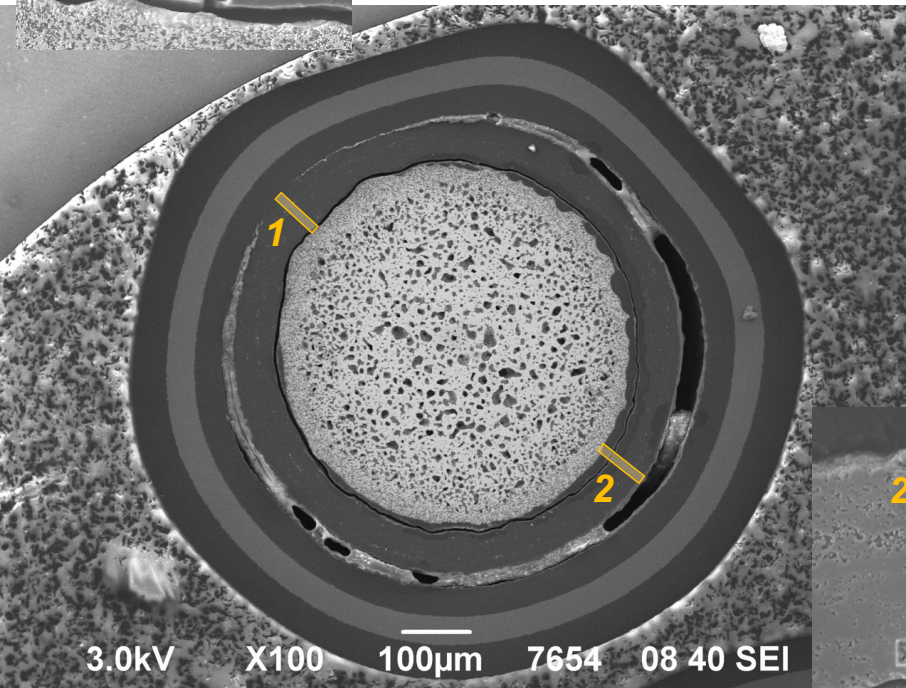
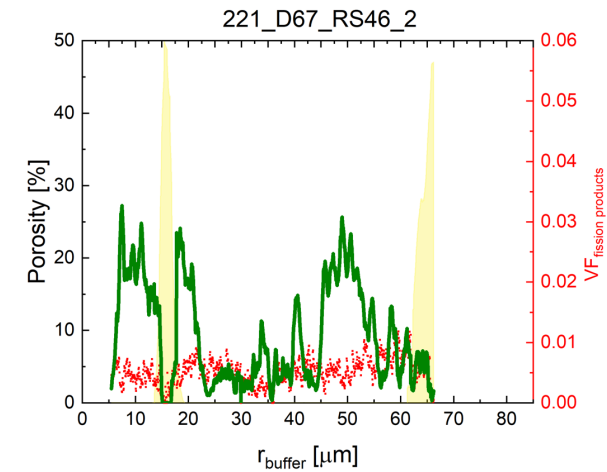
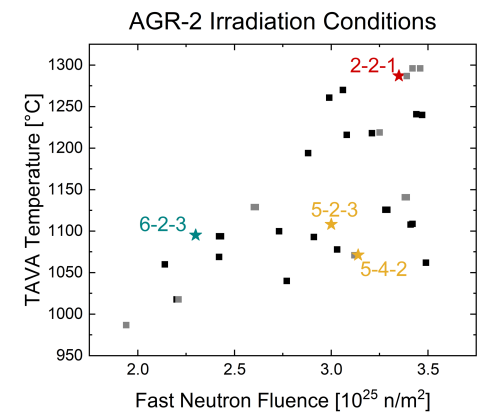
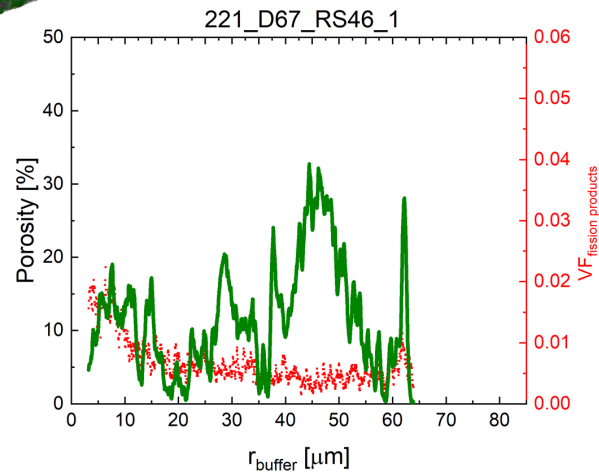
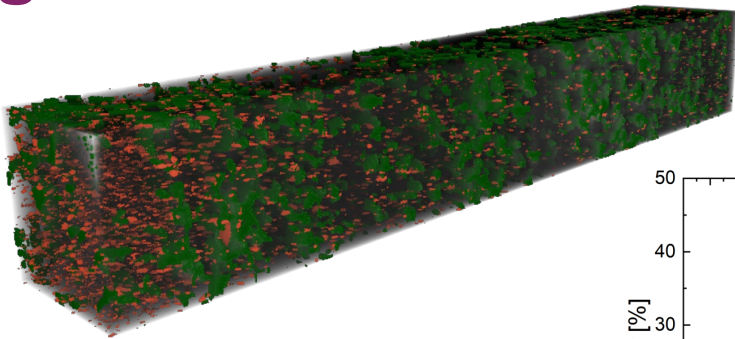
| Compact             | Mount  | Particle | Ag (M_part/M_avg) | Temperature [°C] | Fluence [ $10^{25}$ n/m <sup>2</sup> ] | #full buffer scans | Raman | TEM |
|---------------------|--------|----------|-------------------|------------------|--|--------------------|-------|-----|
| 221                 | MM-D67 | RS43     | 1.12              | 1287             | 3.35                                   | 2                  | X     | X   |
| 221                 | MM-D67 | RS46     | 1.8               | 1287             | 3.35                                   | 2                  |       | X   |
| 221                 | MM-D68 | RS39     | 0.83              | 1287             | 3.35                                   | 1                  |       |     |
| 523                 | MM-D12 | RS11     | 0.48              | 1108             | 3.00                                   | 1                  |       | X   |
| 523                 | MM-D12 | RS28     | 0.43              | 1108             | 3.00                                   | 1                  |       |     |
| 542                 | MM-D55 | RS25     | 1.59              | 1071             | 3.14                                   | 2                  | X     |     |
| 623                 | MM-D69 | RS18     | 1.87              | 1095             | 2.30                                   | 2                  |       | X   |
| 623                 | MM-D69 | RS07     | 1.72              | 1095             | 2.30                                   | 1                  |       | X   |
| 623                 | MM-D70 | RS35     | 0.81              | 1095             | 2.30                                   | 1                  | X     | X   |
| As fabricated AGR-2 |        |          | N/A               |                  |  | 1                  | X     | X   |



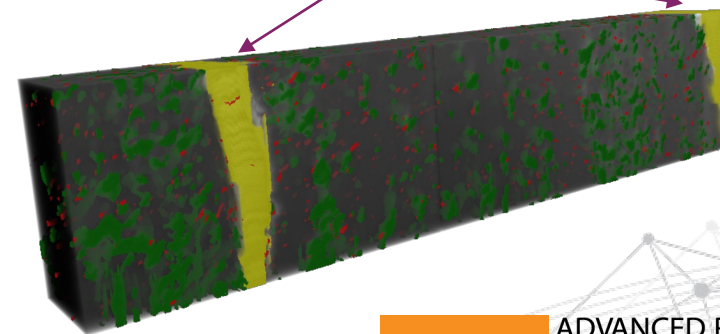
# Example: Capsule 2, high temperature and high fluence



D67-RS46

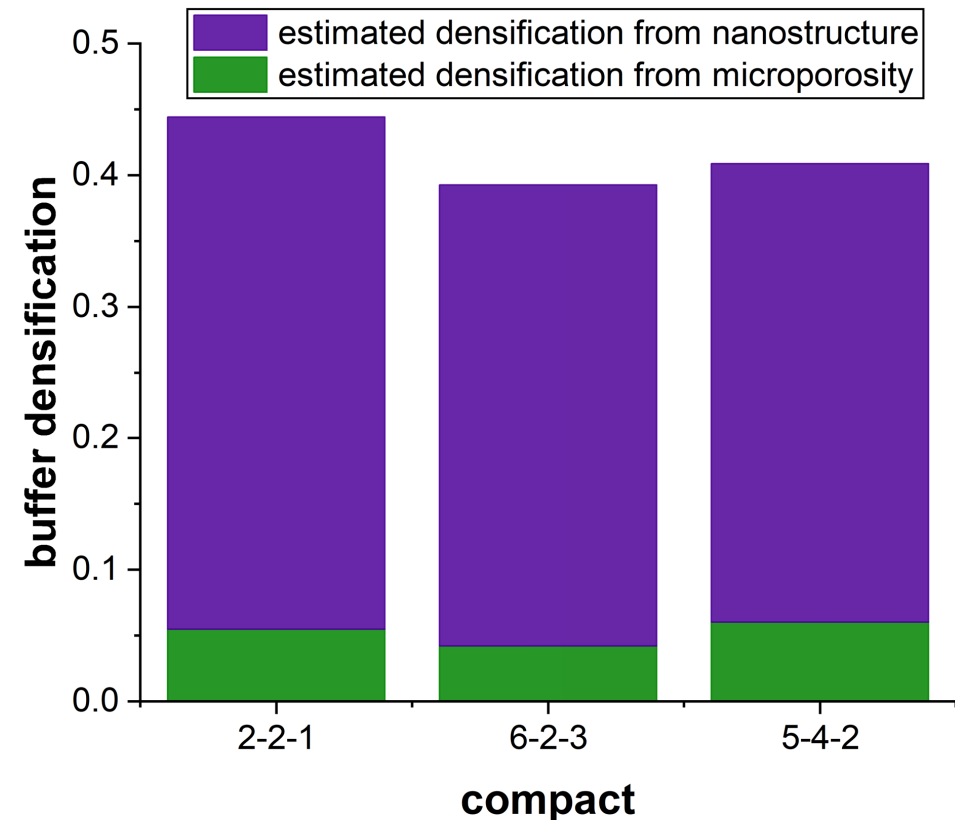
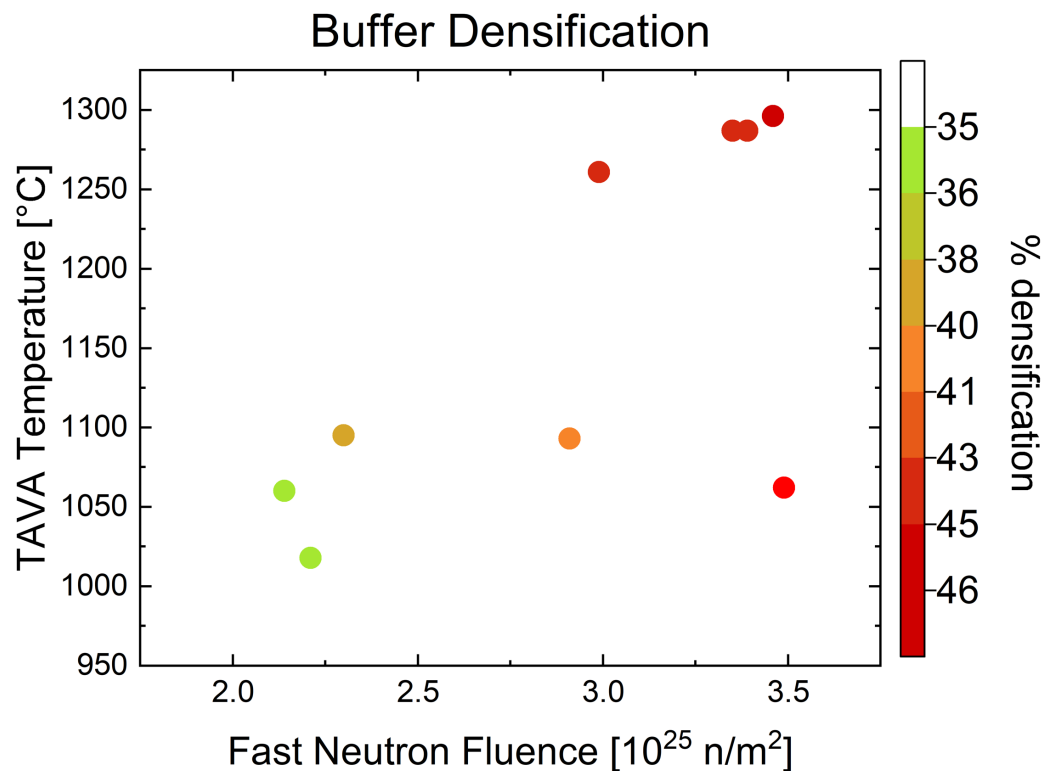


Crack



# Buffer densification: Change in matrix & porosity

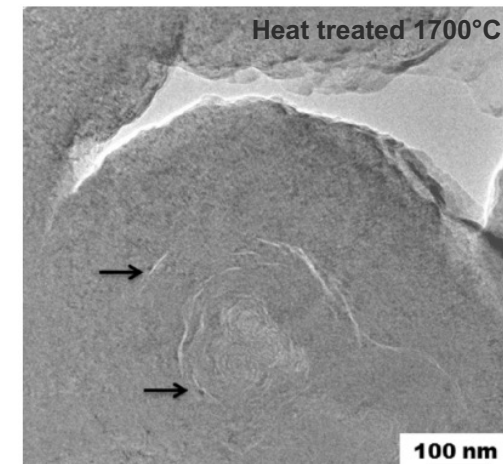
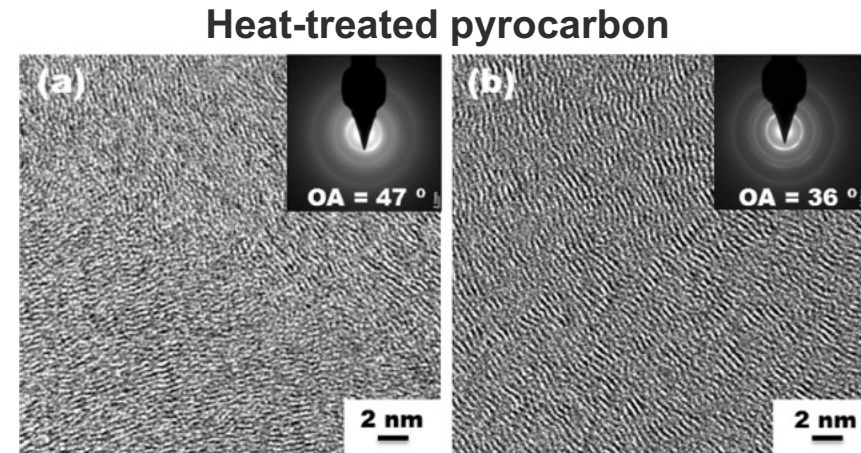
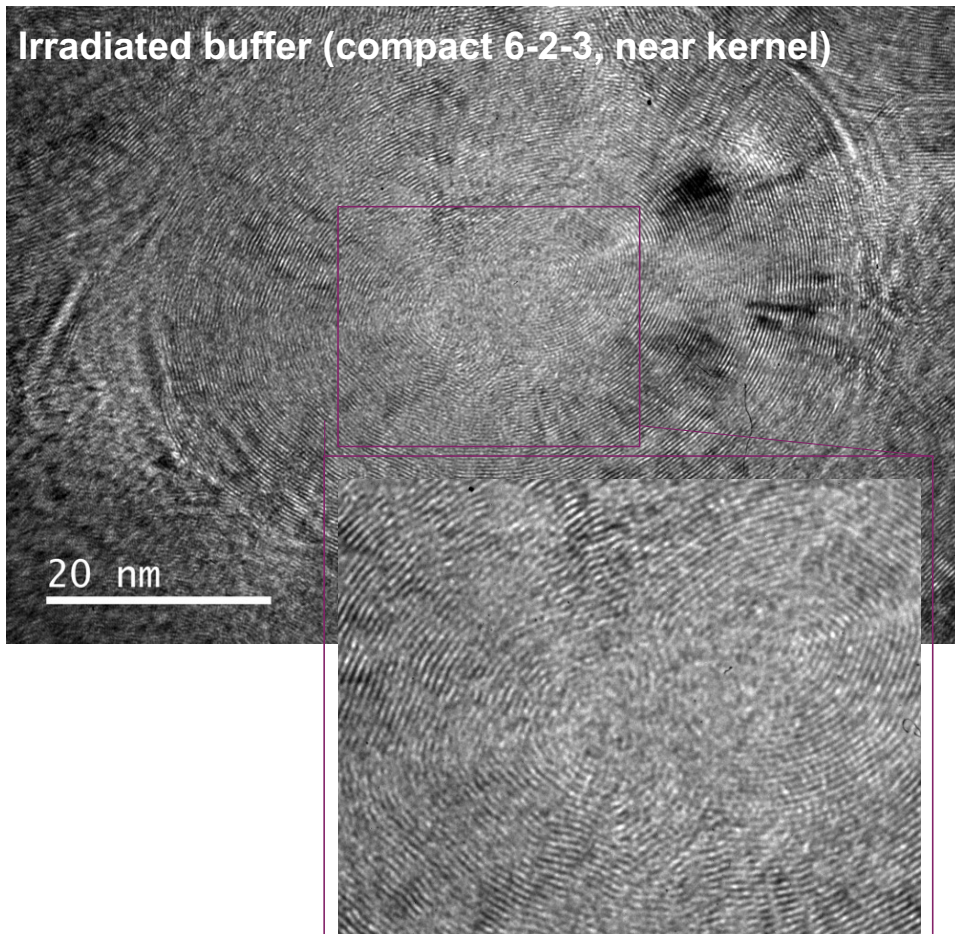
- Substantial densification that correlate positively with fluence and temperature has been observed and found to be dominated by change in matrix microstructure.
- Irradiation changes the average porosity, its local fluctuation and radial distribution.
- The matrix has experienced substantial graphitization as suggested by XRD and Raman analyses.





# Change in matrix microstructure: formation of unique graphitic onion-like nanostructures from TEM

- Formation of onion-like nanostructure (left) characterized by TEM. The feature is similar to that has been observed in heat-treated non-textured pyrocarbon (right).



Cancino-Trejo et al, Carbon (2016)





# Super-elasticity of unirradiated buffer pyrocarbon

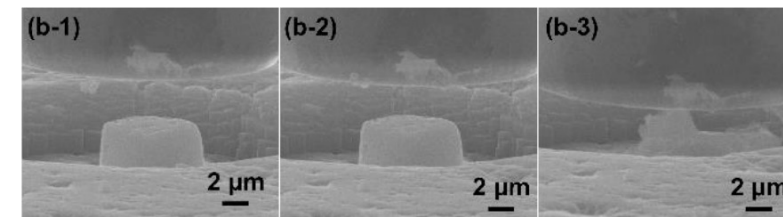
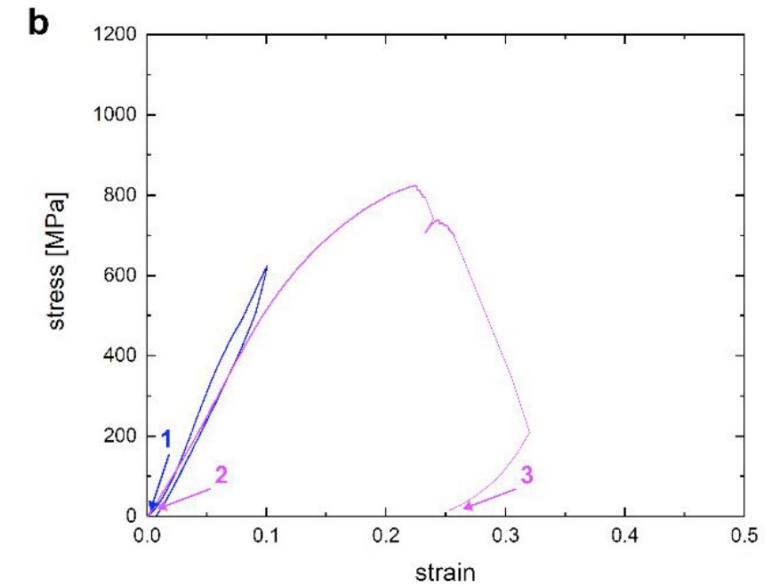
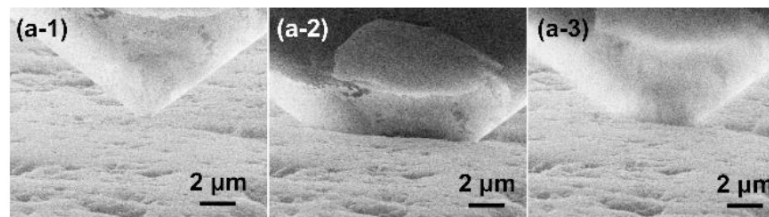
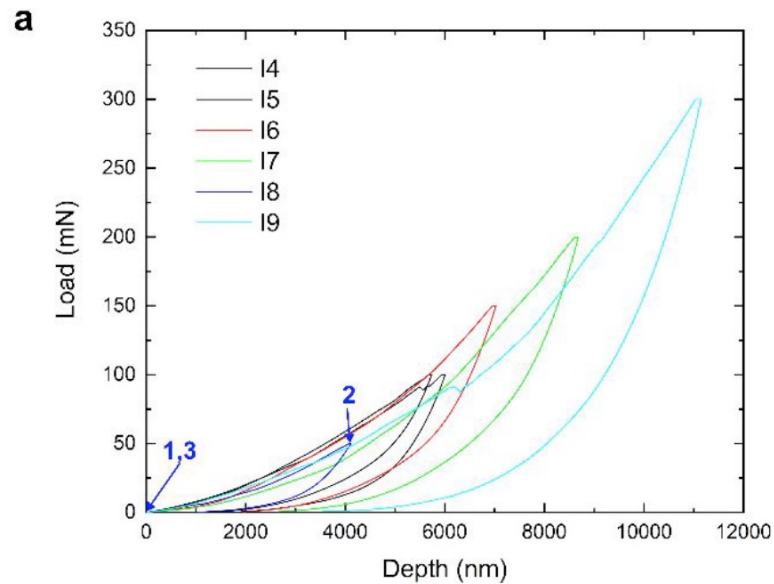
## Nanoindentation and micro-compression

- *C. Griesbach, T. Gerczak, Y. Zhang, R. Thevamaran, Super elasticity and anisotropic mechanical response in porous pyrocarbon (in preparation)*

# Super-elasticity revealed by nanoindentation and nano-pillar compression

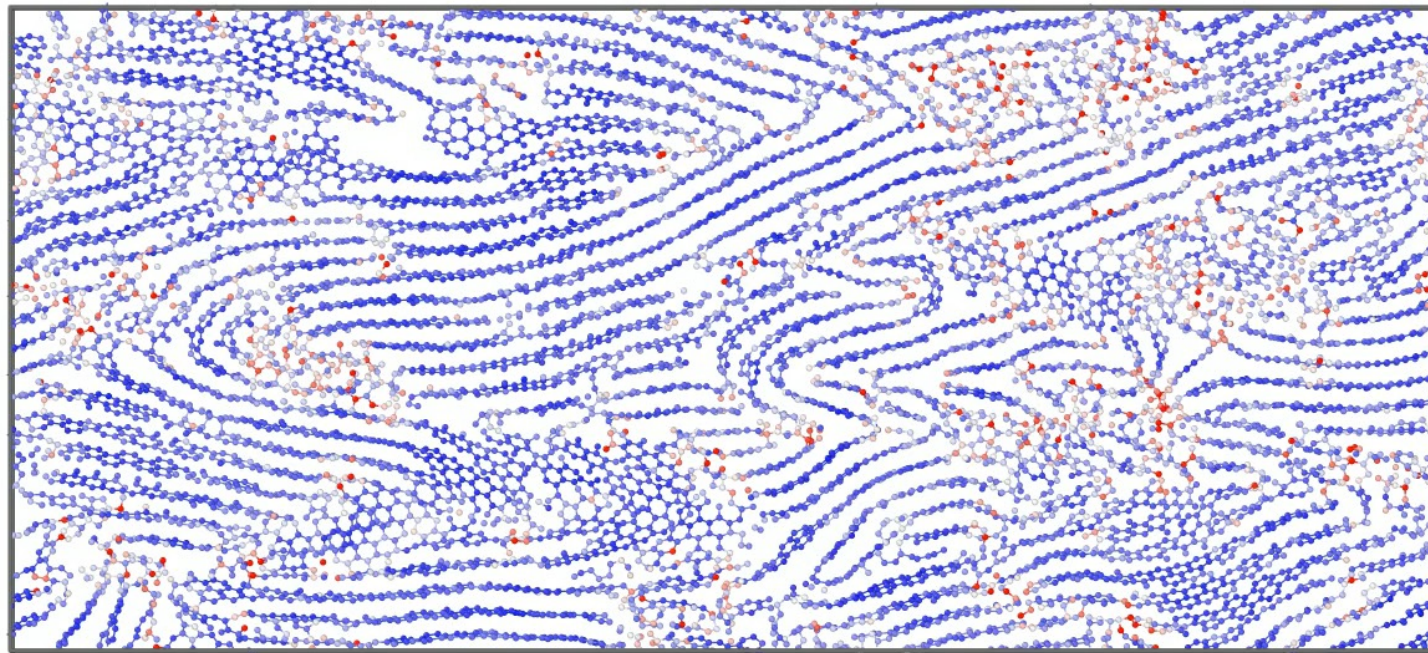
- No failure or plasticity observed during in-situ nanoindentation.
- Brittle failure observed until 30% strain under micro-compression
- Radially compressed micro-pillar show lower yield strength than tangentially compressed.

(a) force-displacement curves from in situ SEM nanoindentation experiments with SEM images at select points during deformation in (a-1) – (a-3), (b) stress-strain curves from in situ SEM micro-compression experiments on the same sample compressed to ~10% strain without yielding (blue curve) and to ~30% strain exhibiting brittle failure; SEM images at select points during deformation in (b-1) – (b-3).



# The super-elasticity is related to the unique way of non-textured pyrocarbon for accommodating strain

- Non-textured pyrocarbon can sustain large tensile and compressive strain.
- The stress and plastic deformation (bond breaking and forming) are most accommodated by the disordered regions between 'crystallites' (graphite-like regions).
- The crystallites grows and align with each other along the loading direction, enhancing texture.



Atomic stress



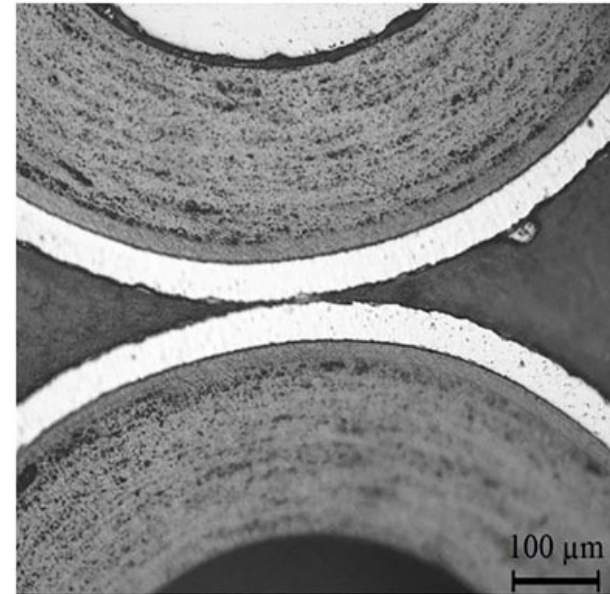
Low

high



# Outlook

- **Can we optimize the fracture behavior by controlling the initial buffer microstructure and porosity distribution?**
  - **Anisotropic porosity distribution and mechanical properties**
  - **Atomic-scale mechanisms responsible for irradiation induced change in matrix microstructure and porosity distribution, which determine the transient mechanical properties**
  - **Progression of buffer fracture into SiC layer**
- **A Letter Of Intent (LOI) has been submitted for phase-II continuation.**



## Summary

- Buffer consists of a low density pyrocarbon matrix (~58% theoretical density) and randomly distributed pores with a total volume of about 14%. The porosity increase radially and fluctuate locally.
- The radial porosity distribution strongly affects the fracture behavior of buffer.
- Irradiation causes significant densification and changes the total porosity, the porosity distribution, and the matrix microstructure. The densification is dominated by the graphitization of the pyrocarbon matrix.
- The unirradiated buffer pyrocarbon exhibits super-elasticity under compression. The strain is accommodated by bending and reorientation of graphite crystallites.
- The findings suggest the possibility of optimizing the fracture behavior by controlling the initial buffer microstructure.



# Thank you!



# Project information: Statistical modeling of the effect of microstructural heterogeneity on the irradiation behavior of TRISO fuel buffer layer

- PI: Yongfeng Zhang, University of Wisconsin Madison (UW)
- Co-PIs: Ramathasan Thevamaran (UW), Karim Ahmed (TAMU), Tyler Gerczak (ORNL), Wen Jiang (INL)
- Funding: \$800,000
- Period: 10/1/2020 – 9/30/2023 (with NCE to 6/30/2024)
- Milestones: (Accomplished in green; M2 in bold)
  1. (M3) TRISO buffer pyrocarbon sample delivery and preparation memo, 9/30/2021
  2. **(M2) Year 1 Annual Progress Report, 9/30/2021**
  3. (M3) Phase field modeling of pyrocarbon fracture with pores, 9/30/2022
  4. (M3) BISON model development for TRISO particle, 9/30/2022
  5. **(M2) Year 2 Annual Progress Report, 9/30/2022**
  6. (M3) Pore structure characterization in TRISO buffer, 12/31/2022
  7. (M3) BISON statistical modeling of buffer tearing, 6/30/2024
  8. (M3) Mechanical property measurement in TRISO buffer, 6/30/2024
  9. **(M2) Final Project Report, 9/30/2024**